Hygroscopic properties of volcanic ash

T. L. Lathem,[1] P. Kumar,[2] A. Nenes,[1,2] J. Dufek,[1] I. N. Sokolik,[1] M. Trail,[3] and A. Russell[3]

[1] Limited observational data exists on the physical interactions between volcanic ash particles and water vapor; yet it is thought that these interactions can strongly impact the microphysical evolution of ash, with implications for its atmospheric lifetime and transport, as well as formation of water and ice clouds. In this study, we investigate for the first time, the hygroscopic properties of ultra-fine volcanic ash (<125 μm diameter) from the eruptions of Mt. St. Helens in 1980, El Chichón in 1982, Tungurahua in 2006, Chaitén in 2008, Mt. Redoubt in 2009, and Eyjafjallajökull in 2010. The hygroscopicity of the ash particles is quantified by their ability to uptake water and nucleate into cloud drops under controlled levels of water vapor supersaturation. Evidence presented strongly suggests that ash uptakes water efficiently via adsorption and a simple parameterization of ash hygroscopicity is developed for use in ash plume and atmospheric models. **Citation:** Lathem, T. L., P. Kumar, A. Nenes, J. Dufek, I. N. Sokolik, M. Trail, and A. Russell (2011), Hygroscopic properties of volcanic ash, *Geophys. Res. Lett.*, *38*, L11802, doi:10.1029/2011GL047298.

1. Introduction

[2] Explosive volcanic eruptions release large quantities of ash particles and gases into the atmosphere, which can be transported over long distances and have a strong influence on the environment and climate [*Sparks et al.*, 1997; *Schumann et al.*, 2010]. Ash impacts are largely determined by complex microphysical processes that are challenging to study in-situ [e.g., *Schumann et al.*, 2010; *Hobbs et al.*, 1981], so most knowledge on plume composition and size distribution comes from post-eruption analysis of ash deposits. Considerable uncertainties remain on the concentration and size distribution of particles emitted by volcanoes, as well as their microphysical interactions [*Textor et al.*, 2006; *Delmelle et al.*, 2007].

[3] Ash particles are usually highly angular shards of amorphous glass produced during fragmentation or comminution, with a majority ranging from nm to mm in size [*Dufek and Manga*, 2008; *Heiken and Wohletz*, 1985]. Ash composition reflects that of the source magma, ranging from rhyolitic (high silica content) to basaltic (low silica content). Siliceous volcanic ash can also contain crystal shards from the primary magma, lithic materials from the volcanic conduit margins, and salts formed in the eruptive column or entrained remnants of brines from hydrothermal systems [*Delmelle et al.*, 2007]. These salts can be hygroscopic and increase the ability of ash to uptake water vapor, which is the dominant gas emitted during most explosive volcanic eruptions [*Textor et al.*, 2006]. Water vapor concentrations can increase further from the upward transport of evaporated groundwater or glacial ice and from the entrainment of moist environmental air [*Herzog et al.*, 1998]. If water vapor concentration is high enough to form liquid coatings on ash, important implications arise for the aggregation, atmospheric lifetime, and detection ability of the ash [*Prata et al.*, 2001; *Textor et al.*, 2006]. Furthermore, activation of ash into cloud droplets or formation of ice crystals can notably increase plume temperature and buoyancy through latent heat release [*Herzog et al.*, 1998], as well as indirectly affect climate by contributing cloud condensation nuclei (CCN) and ice nuclei (IN) [*Seinfeld and Pandis*, 2006].

[4] The occurrence of wetted ash aggregates and frozen hydrometeor fallout is observational proof of ash-water interactions [*Sparks et al.*, 1997; *Hobbs et al.*, 1981], yet limited data exists to quantify the ability of ash to uptake water vapor. *Delmelle et al.* [2005] performed high resolution N_2 and H_2O adsorption-desorption experiments on six different volcanic samples. All samples exhibited high specific surface areas, were more reactive towards H_2O than N_2, and formed a monolayer of H_2O at 0.05–20 % relative humidity. This lead to the assumption in many microphysical studies that ash is always covered by a liquid layer [e.g., *Textor et al.*, 2006]. However, the high temperature and strong competition for water vapor among the high concentration of ash particles in the plume may deplete the supersaturation, so that few (if any) particles can have complete coverage of water, especially in the near vent region. In this study, we comprehensively characterize ash-water interactions over a wide range of water vapor saturations, using CCN activity measurements of samples collected from a variety of recent eruptions. We then determine the physics governing the observed hygroscopicity and develop a parameterization for use in plume microphysical and atmospheric models.

2. Experimental Methods

[5] Ground samples of volcanic ash were collected from the eruptions of Mt. St. Helens (1980), El Chichón (1982), Tungurahua (2006), Chaitén (2008), Mt. Redoubt (2009), and Eyjafjallajökull (2010) and were selected to encompass a wide range of location, composition, crystallinity and eruptive style. All samples were collected near the volcano with the exception of Mt. Redoubt (~130 km downwind). The ash was collected within two days of the eruption for Mt. St. Helens, El Chichón, and Mt. Redoubt. Tungurahua, Chaitén, and Eyjafjallajökull samples were each collected

[1]School of Earth and Atmospheric Sciences, Georgia Institute of Technology, Atlanta, Georgia, USA.
[2]School of Chemical and Biomolecular Engineering, Georgia Institute of Technology, Atlanta, Georgia, USA.
[3]School of Civil and Environmental Engineering, Georgia Institute of Technology, Atlanta, Georgia, USA.

Table 1. FHH Adsorption Model Parameters and Exponent Comparisons Determined for Analyzed Volcanic Ash Samples

Sample[a]	Location	Sample Latitude and Longitude	Sample Age	A_{FHH}	B_{FHH}	x_{exp}	x_{FHH}
Eyjafjallajökull (2010)	Iceland	63.546, −19.662	3 weeks	0.74	1.09	−0.96	−0.96
Mt. Redoubt (2009)	Alaska, USA	59.435, −151.709	2 days	1.05	0.94	−1.14	−1.09
Chaitén (2008)	Chile	−42.814, −72.646	1 month	1.87	1.41	−0.89	−0.90
Tungurahua (2006)	Ecuador	−1.518, −78.488	28 months	2.96	1.42	−0.83	−0.87
El Chichón (1982)	Mexico	17.360, −93.228[b]	2 days	2.91	1.27	−0.76	−0.84
Mt. St. Helens (1980)	Washington, USA	46.232, −122.152	29 years	3.00	1.36	−0.74	−0.85
Mt. St. Helens (1980)	Washington, USA	46.248, −122.178[b]	2 days	3.00	1.29	−0.76	−0.85

[a]Eruption year in parentheses.
[b]Approximate location.

months after the eruption. The influence of weathering is tested by comparing an original 1980 Mt. St. Helens deposit (collected two days after the eruption) to a sample collected in 2009. Each ash sample is dry sieved to an ultra-fine mode (<125 μm diameter) for subsequent analysis.

[6] Ash hygroscopicity is measured following the methodology of *Kumar et al.* [2011a] and *Moore et al.* [2010]. Ash aerosol is generated by placing three grams of dry ash in a 1000 mL sealed Erlenmeyer flask connected to a Burrell Wrist Action Shaker (Model 75). Filtered air flows into the shaking flask that generates dry, polydisperse aerosol by mechanically dispersing the ash particles. The dry ash aerosol is sent to a Differential Mobility Analyzer (DMA, TSI Model 3081) for size classification by electrical mobility (with sheath flow 2.3 L min^{-1} and aerosol flow 0.45 L min^{-1}). The DMA outputs monodisperse aerosol that is then split and sent to a Condensation Particle Counter (CPC, TSI Model 3010), that measures the total concentration of particles (CN), and a Droplet Measurement Technologies Continuous Flow Streamwise Thermal Gradient CCN chamber (DMT CFSTGC) [*Roberts and Nenes*, 2005] for measuring the concentration of particles that act as cloud condensation nuclei (CCN) over a range (0.2% to 1.0%) of water vapor supersaturation (SS). SS is controlled in the DMT CFSTGC by varying the flow rate and temperature gradient applied to its growth chamber and is calibrated with an ammonium sulfate (AS) salt standard [*Moore et al.*, 2010].

[7] The voltage applied to the DMA for size selection is changed over time, allowing the sampling of aerosol with diameters between 20 and 850 nm over 180 seconds. Scanning Mobility CCN Analysis (SMCA) [*Moore et al.*, 2010] is then used to invert the data and determine the activation efficiency (CCN/CN ratio) as a function of dry particle size. The effects of particle multiple charging and non-sphericity are accounted for as described by *Moore et al.* [2010] and *Kumar et al.* [2011a]. The resulting dry diameter uncertainty is ±20%, calculated as shown by *Kumar et al.* [2011a] based on an average ash shape factor of 1.3 [*Schumann et al.*, 2010; *Riley et al.*, 2003]. The dry diameter for which 50% of the ash particles act as CCN (for a given SS) in the CFSTGC is called the critical diameter, d_{dry}; any ash particle larger than d_{dry} will act as a CCN.

3. Data Analysis Methodology

[8] Ash hygroscopicity can originate from soluble salts present in the particles, and, from the adsorption of water vapor on the ash surface. The relative importance of each, together with the dry particle size, controls the SS required to form a cloud drop. Köhler theory (KT) can be used to predict SS when soluble salts are the dominant contributor to hygroscopicity [*Seinfeld and Pandis*, 2006]. Solute effects can be parameterized in terms of a "hygroscopicity parameter", κ [*Petters and Kreidenweis*, 2007]. If the ash composition does not vary with size, KT suggests that SS $\sim$ $d_{dry}^{x_{KT}}$, with $x_{KT} \sim -1.5$. Adsorption activation theory (AT) can be used to predict SS when the adsorption of water vapor dominates particle hygroscopicity [*Kumar et al.*, 2009b, 2011a]. The formulation of AT in this study adopts the Frenkel, Halsey and Hill (FHH) adsorption isotherm [*Lowell et al.*, 2004; *Sorjamaa and Laaksonen*, 2007] and uses two empirical parameters, A_{FHH} and B_{FHH}, that are constrained by the CCN experiments. FHH-AT also predicts SS $\sim d_{dry}^{x_{FHH}}$, but x_{FHH} is between −0.8 and −1.1 [*Kumar et al.*, 2009b, 2011a], meaning the slope of SS vs. d_{dry} is less steep than observed for KT.

[9] For each ash sample, SS vs. d_{dry} is fitted to a power law function of the form SS $= Cd_{dry}^{x_{exp}}$, where C and x_{exp} are fitting constants. Additionally, the data are parameterized by FHH-AT [*Kumar et al.*, 2009b, 2011a] to determine the A_{FHH}, B_{FHH} adsorption parameters and x_{FHH}. Comparison of x_{exp} to x_{FHH} and x_{KT} determines which theory (FHH-AT or KT) best describes the observed hygroscopicity of each volcanic ash sample (Table 1).

4. Results and Discussion

[10] Measured SS vs. d_{dry} data are presented in Figure 1 for all samples considered. Ash samples are denoted by points, and the FHH-AT model fits to the data are shown as solid lines. Results for ammonium sulfate salt are shown as a reference for KT. Black dashed lines indicate lines of constant κ, and are used to gauge the ash hygroscopicity. Figure 1 demonstrates that volcanic ash is hygroscopic and CCN active, even at atmospherically relevant SS. Despite large variations in composition and eruptive dynamics, the activation data for ash are quite consistent, and have a lower hygroscopicity than what *Kumar et al.* [2011a] observed for atmospheric mineral dust aerosol and clays (with most ash $\kappa \leq 0.03$ and most dust $\kappa \leq 0.05$). The lower apparent hygroscopicity of volcanic ash relative to dust originates from differences in water adsorption capacity arising from differences in molecular structure. Consistent with *Bolis et al.* [1985], the water adsorption capacity of crystalline quartz (present in dust) is greater than the water adsorption of amorphous silica (present in volcanic ash). The sole exception is Mt. Redoubt ash, which exhibits an average apparent $\kappa \sim 0.15$, which is higher than any other dust or ash samples studied to date. This could be the result of more complex particle morphology or size dependent composition. For example, an enrichment of solute (salts) in the
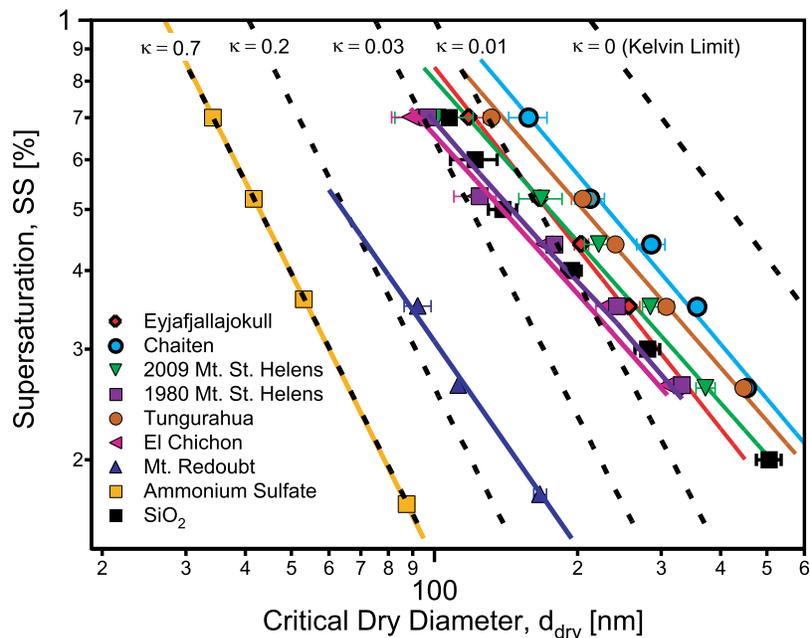
Figure 1. CCN activation data, supersaturation vs. critical dry diameter, for the different volcanic ash samples presented in Table 1. Solid symbols represent the ash samples, with errors bars showing uncertainty in the critical dry diameter. Solid lines represent FHH adsorption activation theory fits, while dashed lines represent values of constant κ-Köhler hygroscopicity, ranging from completely insoluble ($\kappa = 0$) to highly soluble ($\kappa = 0.7$).

ultra-fine Redoubt ash of up to 20% volume fraction would be sufficient to explain a $\kappa \sim 0.15$, therefore it is possible the hygroscopicity of Redoubt ash is a combination of KT and FHH-AT [*Kumar et al.*, 2011a, 2011b].

[11] A comparison of the slopes of SS vs. d_{dry} (Figure 1) reveals slopes that deviate significantly from classical KT behavior (SS $\sim d_{dry}^{-1.5}$), suggesting that solute does not contribute substantially to the observed ash hygroscopicity. In fact, the CCN activity of the volcanic ash samples can be well represented by the FHH-AT model fits (Figure 1, solid lines) and is consistent with the study of *Delmelle et al.* [2005]. Bulk Ion Chromatography (IC) analysis of all ash samples (not shown) further supports adsorption as the dominant mechanism, as all soluble ions (at less than 0.5% by mass), are not sufficient to explain the observed hygroscopicity. Additionally, the similarity between Mt. St. Helens 1980 and 2009 samples (agreement of x_{exp} in Table 1 to within 3%) suggests that weathering does not significantly alter the observed activation behavior.

[12] For all volcanic ash samples, FHH-AT represents the observed CCN activity (x_{exp}) to within 12% (Table 1). This results in an average $A_{FHH} = 2.22 \pm 0.99$ and a $B_{FHH} = 1.25 \pm 0.18$, with uncertainty including the influence of particle non-sphericity. Excluding the Mt. Redoubt sample, $A_{FHH} = 2.41 \pm 0.93$ and a $B_{FHH} = 1.31 \pm 0.12$. As shown by *Kumar et al.* [2009b, 2011a], the B_{FHH} adsorption parameter dominates the activation physics, with A_{FHH} of secondary importance. Therefore, the relatively small variation in B_{FHH} among a variety of volcanic eruptions is encouraging for future modeling applications and suggests that this simple parameterization of adsorption could be applied for all volcanic ash.

[13] Measurement of subsaturated ash water uptake (e.g., with Hygroscopic Tandem Differential Mobility Analysis; HTDMA) can be used to further test the robustness of

FHH-AT because it predicts a considerably different growth response than KT [e.g., *Kumar et al.* [2009a]. For example, using FHH-AT parameters from CCN activity measurements (Table 1) and assuming 90% relative humidity (i.e., $S = 0.9$), Mt. Redoubt ash grows 5 ± 1 % relative to its dry diameter. If the same particles follow KT with $\kappa = 0.15$, a much larger growth is anticipated, about 31 ± 1 %. The other ash samples would generally exhibit smaller humidified growth, between 2 and 5 % at $S = 0.9$. A future study will focus on hygroscopic closure against these predictions.

5. Conclusions

[14] In this study, the hygroscopicity of ash aerosol generated from in-situ deposits of six different volcanic eruptions is experimentally quantified and, for the first time, a simple parameterization for ash-water interactions is provided. A combination of CCN activation data and IC analysis suggests adsorption of water vapor onto the ash surface gives rise to the observed hygroscopicity. This work confirms that the surface of insoluble ash particles efficiently adsorbs water as first suggested by *Delmelle et al.* [2005]. Despite large variations in ash composition across samples, a single set of adsorption parameters ($A_{FHH} = 2.41 \pm 0.93$ and $B_{FHH} = 1.31 \pm 0.12$) can describe the ash hygroscopicity with sufficient accuracy for use in volcanic plume and atmospheric climate models, with the end goal to improve predictions of ash microphysics, transport and impacts.

References

Bolis, V., B. Fubini, S. Coluccia, and E. Mostacci (1985), Surface hydration of crystalline and amorphous silicas, *J. Therm. Anal.*, *30*, 1283–1292.

Delmelle, P., F. Villiéras, and M. Pelletier (2005), Surface area, porosity and water adsorption properties of fine volcanic ash particles, *Bull. Volcanol.*, *67*, 160–169.

Delmelle, P., M. Lambert, Y. Dufrêne, P. Gerin, and N. Óskarsson (2007), Gas/aerosol–ash interaction in volcanic plumes: New insights from surface analyses of fine ash particles, *Earth Planet. Sci. Lett.*, *259*, 159–170.

Dufek, J., and M. Manga (2008), In situ production of ash in pyroclastic flows, *J. Geophys. Res.*, *113*, B09207, doi:10.1029/2007JB005555.

Hobbs, P. V., L. F. Radke, M. W. Eltgroth, and D. A. Hegg (1981), Airborne studies of the emissions from the volcanic eruptions of Mount St. Helens, *Science*, *211*, 816–818.

Heiken, G., and K. H. Wohletz (1985) *Volcanic Ash*, 245 pp., Univ. of Calif. Press, Berkeley.

Herzog, M., H–F. Graf, C. Textor, and J. M. Oberhuber (1998), The effect of phase changes of water on the development of volcanic plumes, *J. Volcanol. Geotherm. Res.*, *87*, 55–74.

Kumar, P., A. Nenes, and I. N. Sokolik (2009a), The importance of adsorption for CCN activity and hygroscopic properties of mineral dust aerosol, *Geophys. Res. Lett.*, *36*, L24804, doi:10.1029/2009GL040827.

Kumar, P., I. N. Sokolik, and A. Nenes (2009b), Parameterization of cloud droplet formation for global and regional models: Including adsorption activation from insoluble CCN, *Atmos. Chem. Phys.*, *9*, 2517–2532.

Kumar, P., I. N. Sokolik, and A. Nenes (2011a), Measurements of cloud condensation nuclei activity and droplet activation kinetics of fresh unprocessed regional dust samples and minerals, *Atmos. Chem. Phys.*, *11*, 3527–3541.

Kumar, P., I. N. Sokolik, and A. Nenes (2011b), Measurements of cloud condensation nuclei activity and droplet activation kinetics of wet processed regional dust samples and minerals, *Atmos. Chem. Phys. Discuss.*, *11*, 12,561–12,605.

Lowell, S., J. E. Shields, M. A. Thomas, and M. Thommes (2004), *Characterization of Porous Solids and Powders: Surface Area, Pore Size and Density*, Kluwer Acad., Dordrecht, Netherlands.

Moore, R. H., A. Nenes, and J. Medina (2010), Scanning mobility CCN analysis—A method for fast measurements of size resolved CCN distributions and activation kinetics, *Aerosol Sci. Technol.*, *44*, 861–871.

Petters, M. D., and S. M. Kreidenweis (2007), A single parameter representation of hygroscopic growth and cloud condensation nucleus activity, *Atmos. Chem. Phys.*, *7*, 1961–1971.

Prata, F., G. Bluth, B. Rose, D. Schneider, and A. Tupper (2001), Comments on "Failures in detecting volcanic ash from satellite-based tecnhique", *Remote Sens. Environ.*, *78*, 341–346.

Riley, C. M., W. I. Rose, and G. J. S. Bluth (2003), Quantitative shape measurements of distal volcanic ash, *J. Geophys. Res.*, *108*(B10), 2504, doi:10.1029/2001JB000818.

Roberts, G., and A. Nenes (2005), A continuous-flow streamwise thermal-gradient CCN chamber for atmospheric measurements, *Aerosol Sci. Technol.*, *39*, 206–221.

Seinfeld, J., and S. Pandis (2006), *Atmospheric Chemistry and Physics: From Air Pollution to Climate Change*, 2nd ed., John Wiley, New York.

Schumann, U., et al. (2010), Airborne observations of the Eyjafjalla volcano ash cloud over Europe during air space closure in April and May 2010, *Atmos. Chem. Phys. Discuss.*, *10*, 22,131–22,218.

Sorjamaa, R., and A. Laaksonen (2007), The effect of H_2O adsorption on cloud drop activation of insoluble particles: A theoretical framework, *Atmos. Chem. Phys.*, *7*, 6175–6180.

Sparks, R. S. J., et al. (1997), *Volcanic Plumes*, 574 pp., John Wiley, Chichester, U. K.

Textor, C., H. F. Graf, M. Herzog, J. M. Oberhuber, W. I. Rose, and G. G. J. Ernst (2006), Volcanic particle aggregation in explosive eruption columns. Part I: Parameterization of the microphysics of hydrometeors and ash, *J. Volcanol. Geotherm. Res.*, *150*, 359–377.

J. Dufek, T. L. Lathem, A. Nenes, and I. N. Sokolik, School of Earth and Atmospheric Sciences, Georgia Institute of Technology, Atlanta, GA 30332, USA. (terry.lathem@eas.gatech.edu)

P. Kumar, School of Chemical and Biomolecular Engineering, Georgia Institute of Technology, Atlanta, GA 30332, USA.

A. Russell and M. Trail, School of Civil and Environmental Engineering, Georgia Institute of Technology, Atlanta, GA 30332, USA.